UFSM

REGET/UFSM
Revista Eletrônica em Gestão, Educação e Tecnologia Ambiental

V. 26 2022

ISSN 2236-1170
Acesso aberto

REGET, v. 26, e10, 2022 • https://doi.org/10.5902/2236117066989
Submitted: 30/07/2021 • Accepted: 07/12/2022 • Published: 17/01/2023

Environmental Technology

Association of advanced oxidative and adsorptive processes for dye treatment in the sanitizer industry: kinetic, equilibrium and toxicity evaluation

Daniella Carla Napoleão [I], Tássia Santos Gonçalves [I], Naiana Santos da Cruz Santana Neves[I], Vanessa de Oliveira Marques Cavalcanti[I], Marina Gomes Silva[I], Ingrid Larissa da Silva Santana[I], Rayany Magali da Rocha Santana[I], Alex Leandro Andrade de Lucena[I], Graziele Elisandra do Nascimento[I]

[I] Universidade Federal de Pernambuco, Recife, PE, Brazil

ABSTRACT

The presence of dyes in wastewater can cause several damages to the environment. Aiming at its removal, advanced oxidative processes (AOP) and adsorption (ADS) have been used. In this work, the removal of acid blue dye 80 (AA80) by AOP (photoperoxidation (PP) and photo-Fenton (PF)) and by ADS was evaluated, individually and combined. The use of the PP/UV-C system led to degradations of 72.7 and 83.8% for the λ of 334 and 622 nm, respectively. The PP/LED system did not degrade. For the PF process, > 90% degradation was obtained for both radiations. The [Fe] (1 mg L^{-1}) and H_2O_2 concentration ([H_2O_2]) (90 mg L^{-1}) were optimized for the PF/LED system. As for the PP/UV-C system, the optimal [H2O2] was 60 mg L^{-1}. The experimental data fit well with the Chan and Chu (2003) kinetic model with R^2>0.94. The kinetic data showed a better fit to the pseudo-second order model (R^2>0.90), while equilibrium was reached in 30 min with removal of 62.45 (λ=334 nm) and 83.22% (λ=622 nm), being well represented by the Langmuir and Sips models. Finally, the combined study promoted a 7% increase in AA80 removal, achieving an improvement in the final toxicity of the treated matrix when compared to isolated AOP systems.

Keywords: Combined process; Eggshel; LED lamp; UV-C radiation; Seed toxicity

1 INTRODUCTION

Dyes are pigmented chemical substances capable of imparting color to a substrate, being widely applied in the food, pharmaceutical, textile, sanitizing, and other industries (FERRAZ *et al.* 2011; MUTHUPRIYA *et al.* 2016). These substances are categorized according to their chemical class and their intended applications. Among the chemical classes stand out the anthraquinones, which have in its constitutions three conjugated aromatic rings, derived from anthracene, with two carbonyl groups (KIM; CHOI, 2013; DIAZ-MUÑOZ *et al*. 2018).

However, the presence of these compounds in wastewater poses a serious problem. Even at low concentrations, dyes can cause changes in watercolor and therefore cause imbalance in the ecosystem, since their presence blocks the penetration of sunlight, harming the process of photosynthesis of aquatic organisms (RATANAPONGLEKA; PHETSON, 2014; LALNUNHLIMI; KRISHNASWAMY, 2016). Furthermore, according to Selvaraj *et al.* (2021), dyes and their degradation products can be toxic to aquatic life, causing carcinogenic and mutagenic effects to living beings.

Thus, treating surface water is an urgent need; especially when it is verified that the conventional treatments applied in wastewater treatment plants (WWTP) are inefficient in terms of the removal of persistent organic pollutants. Among the alternative treatments used, the advanced oxidation processes (AOP) stand out, as they are capable of mineralizing pollutants, ideally reducing them to CO_2, water, and inorganic salts (BANASCHIK *et al.* 2018). Several types of AOP have been reported in the literature (Fenton, photo-Fenton, photoperoxidation, heterogeneous photocatalysis, ozonation), and the main difference between them is the way in which hydroxyl radicals are generated. These, in turn, are responsible for promoting the degradation of pollutants (GIROLETTI *et al.* 2018).

Among the variables involved in the different systems mentioned above is the use of radiation. Photochemical processes are more efficient than the Fenton process, as the emission of photons accelerates the production of hydroxyl radicals. Therefore,

different types of radiation have been studied over the years. Amorim *et al.* (2020) used AOP photoperoxidation (combined use of radiation and oxidizing agent, in general H_2O_2) and photo-Fenton (use of radiation together with the oxidizing agent and iron ions) to treat the direct red 83 textile dye employing bench reactors with ultraviolet (UV) and sunlight. The authors found greater treatment efficiency by combining the photoperoxidation process with UV-C radiation. Ramos *et al.* (2020) studied the degradation of the indigo carmine dye using the Fenton, photo-Fenton, photoperoxidation and direct photolysis processes. In this work it was found that the photo-Fenton process with UV-C radiation was the most efficient in terms of mineralization of the dye under study.

However, it is known that the use of UV radiation can increase the costs of the process, making it necessary to evaluate other types of radiation. Moraes *et al.* (2020) mention in their work the importance of evaluating the costs related to the acquisition of lamps, as well as the cost related to the operation of the reactor. Therefore, it is possible to find reports in the literature on the application of LED radiation in the use of AOP (XIONG *et al.* 2020). Yin; Shang (2020) used AOP UV-LED/chlorine followed by adsorption with activated carbon to treat the micropollutants bisphenol A, diclofenac and caffeine. Another alternative to improve the treatment efficiency is the combined use of AOP and adsorptive processes.

The adsorption is an efficient process for the removal of organic compounds, standing out for its easy operation, low energy consumption, simple methodology and the possibility of using residues to produce adsorptive materials (SALLES *et al.* 2022, BRUCKMANN *et al.* 2022). The use of these materials becomes favourable in view of their high availability, accessible and sustainable processing, in addition to the great diversity of agro-industrial residues that can be used (VIDOVIX *et al.* 2022, BABAKIR; ALI; ISMAIL, 2022). The literature shows the use of the most diverse types of waste (WANG *et al.* 2018; MEILI *et al.* 2019; GHIBATE; SENHAJI; TAOUIL, 2021) used to treat toxic substances and their by-products. In this way, eggshell stands out as a good adsorbent,

being a natural material composed of a variety of functional groups such as -OH, -NH_2, -COOH, on its surface, enabling affinity with dyes (HEVIRA *et al.* 2020; WU *et al.* 2022).

The justification for the combined use of such processes is due to the fact that in some cases the use of AOP can lead to the formation of intermediate compounds (by-products) that increase the toxicity of the treated solution when compared to the initial solution. It is suggested that these by-products can be better adsorbed than the original compounds, due to the lower complexity of their structures.

Considering the possible formation of intermediates, investigating the toxicological power that the application of AOP can cause is essential, as it is known that persistent organic pollutants can cause carcinogenic and mutagenic effects (BORTOTI *et al.* 2016). Tests have been carried out with different organisms, namely: fish, vegetable seeds, bacteria and microcrustaceans (PRIAC *et al.* 2017).

Given the above, the objective of this work was to treat the acid blue dye 80, using advanced oxidation processes and adsorptive processes in an isolated and combined way, aiming at a complete elimination of the pollutant and possible intermediates formed.

2 EXPERIMENTAL

2.1 Identification and quantification of the acid blue dye 80

An aqueous solution of the acid blue 80 dye (Colour Index 61585, molecular formula $C_{32}H_{28}N_2Na_2O_8S_2$ and molar mass of 678.682 g mol^{-1}) with a concentration of 15 mg L^{-1} (working solution) was used. To determine their characteristic wavelengths (λ), spectral scanning from 200 to 800 nm was performed in an ultraviolet/visible (UV/Vis) spectrophotometer (Thermoscientific).

Then, to quantify the dye in the solution before and after treatment, analytical curves were built, with a linear range from 1 to 30 mg L^{-1}, with the limits of quantification (LOD) and detection (LOD), as well as the coefficient of variance (CV) being determined, as described by INMETRO (2016). The spectral behavior of the dye was also analyzed in relation to the pH variation (from 3 to 6) of the solution.

2.2 Advanced oxidation processes: assessment of the influence of variables and kinetic study

Initially, the advanced oxidation processes, photoperoxidation and photo-Fenton were evaluated, in addition to the photolysis process, to identify which, among them, had greater efficiency in the degradation of the dye under study. In the tests, hydrogen peroxide (H_2O_2) (Química Moderna, 30% v/v), was used as an oxidizing agent, $FeSO_4.7H_2O$ (Vetec, 99%), as a catalyst, and a 0.2 mol L^{-1} H_2SO_4 solution for pH adjustment, when applicable. In cases where the use of radiation was necessary, benchtop reactors with UV-C radiation (ZAIDAN *et al.* 2017) and LED (NASCIMENTO *et al.* 2020) were used. The photon emission of each reactor was determined with the aid of radiometers (Instrutherm).

The preliminary tests, in duplicate, were carried out using 50 mL of the working solution, a concentration of H_2O_2 ($[H_2O_2]$) of 100 mg L^{-1} and an exposure time of 60 min. In the execution of the Fenton and photo-Fenton processes, a concentration of iron ([Fe]) equal to 3 mg L^{-1} and a pH in the range of 3-4 was used.

With the results obtained and identified, the AOP with the highest efficiency, for each radiation studied, the univariate study of the parameters influencing the process was carried out. For the photoperoxidation, the $[H_2O_2]$ was varied from 40 to 180 mg L^{-1}. For the photo-Fenton, the optimization of the variables took place in two stages: the first consisted of varying the $[H_2O_2]$ from 40 to 150 mg L^{-1} with fixed [Fe] (3 mg L^{-1}) and the second used the best determined $[H_2O_2]$ and varied the [Fe] in 1, 2, 3, 4 and 5 mg L^{-1}. All tests lasted 60 min and the efficiency of the process was determined from the percentage of degradation. Then, the treatment was evaluated as a function of the volume of solution to be treated, which was varied to 100, 200, 500 and 1000 mL.

Finally, after establishing the best experimental conditions, tests were carried out in order to define the dye degradation kinetics. Thus, the adjustment of the experimental data to the pseudo-first order models proposed by Chan and Chu (2003) (Equation 1 and 2) and He *et al.* (2016) (Equation 3)

$$C = C_0\left(1-\frac{t}{\rho+\vartheta t}\right) \quad (1)$$

$$\frac{t}{1-\frac{C_2}{C_0}} = \rho + \theta t \quad (2)$$

$$-\frac{dC}{dt} = k_r KC = KC \quad (3)$$

Where: ρ represents the reaction kinetics (min) and σ the oxidative capacity of the system (dimensionless), corresponding to the linear coefficient and the angular coefficient of the straight line, respectively. k is the pseudo-first order reaction rate (min^{-1}). C and C_0 are the initial and final dye concentrations (mg L^{-1}) after treatment at a reaction time t (min), respectively.

2.3 Adsorbent preparation and characterization

Chicken eggshell residues were washed with distilled water, then dried in an oven at 80 ± 1 ºC for 24 h. The material was milled in a blender and through a series of Tyler sieves with the following grain size ranges: < 0.09; 0.09 - 0.15; 0.15 - 0.21 nm. The prepared adsorbent was characterized by means of Fourier transform infrared spectroscopy (FTIR) and determination of pH at the point of zero charge (pH_{PZC}).

The FTIR technique was used in order to identify the functional groups present in the developed material. This analysis was performed in a spectral range between 4000 and 500 cm^{-1} in FTIR equipment (Bruker Tensor 27), with an average of 20 scans, spectral resolution of 4 cm^{-1} and attenuated total reflectance (ATR).

To study the pH_{PZC} of the adsorbent, NaOH (0.1 mol L^{-1}) and HCl (0.1 mol L^{-1}) were used to adjust the pH of the dye solution and it was quantified with the aid of a pHmeter (Quimis Q400AS). The test was performed in Erlenmeyer flasks with 25 mL of distilled water, 0.1 g of the adsorbent and pH ranging from 2 to 10. The tests were performed under agitation (300 rpm) on a shaking table (IKE brand, model KS 130 control) for 24 h. Finally, the system was filtered, and the pH of the final solution was quantified. With

the initial and final pH values it was possible to generate a graph with axes (pH_{final} – $pH_{initial}$) versus $pH_{initial}$ and the pH_{PZC} was estimated. With this result, it was possible to start the treatment via adsorption process.

2.4 Factorial design for evaluation of variable of the adsorption process

To define the best working conditions of the adsorptive process to remove the contaminant, a factorial design (2^3) was carried out with a central point in triplicate, totaling 11 independent experiments. The variables and levels (minimum, central and maximum) studied were pH (2, 4 and 6), stirring speed (0, 150, 300 rom) and particle size (< 0.9; 0.9 – 0.15; 0.15 – 0.21 mm). This study was carried out in Erlenmeyer flasks with a capacity of 100 mL, using 25 mL of acid blue 80 dye solution (15 mg L^{-1}), with a fixed mass of 0.2 g of adsorbent, for 180 min.

At the end of the test, the samples were filtered on a white strip filter paper. For statistical analysis, the date obtained was treated in the Statistica 6.0 software, in which Pareto charts were generated. The response variable used was the adsorptive capacity determined from Equation 4.

$$q = \frac{C_0 - C_t}{m} \times V \quad (4)$$

Where q is the adsorptive capacity (mg g^{-1}), C_0 is the initial concentration (mg L^{-1}), C_t is the concentration at a given time point (mg L^{-1}), m is the mass of the biosorbent (g), and V is the solution volume (L). Once the best operational conditions were defined, the kinetic and equilibrium studies of the adsorptive process were carried out.

2.5 Kinetic and equilibrium study of the adsorption process

The kinetic study was carried out under the best conditions defined in the factorial design. Thus, the dye solution was in contact with the biosorbent for 360 min,

with the samples being analyzed at the times of 0, 2, 5, 7, 10, 15, 20, 25, 30, 60, 90, 120, 150, 180, 210, 300 and 360 min.

With the experimental data, the evaluation of the kinetic behavior was carried out using a pseudo-first order (Equation 5) and pseudo-second order (Equation 6) kinetic models.

$$\frac{dq_t}{dt} = k_1(q_e - q_t) \quad (5)$$

$$\frac{dq_t}{dt} = k_2(q_e - q_t)^2 \quad (6)$$

Where k_1 is pseudo-first order adsorption rate constant (min^{-1}), q_e and q_t are the adsorptive capacities (mg g^{-1}) at equilibrium and a given time, respectively. Finally, k_2 is the pseudo-second order adsorption rate constant (g mg^{-1} min^{-1}). For the equilibrium study, dye concentrations ranged from 5 to 100 mg L^{-1}. After obtaining the experimental data, an assessment was made of the adequacy of the Langmuir (Equation 7), Freundlich (Equation 8) and Langmuir-Freundlich (Equation 9) models.

$$q_e = \frac{q_{max} k_L C_e}{1 + k_L C_e} \quad (7)$$

$$q_e = k_F C e^{\frac{1}{n_F}} \quad (8)$$

$$q_e = \frac{q_{max}(k_s C_e)^{1/n_s}}{1 + (k_s C_e)^{1/n_s}} \quad (9)$$

Where: C_e is the equilibrium concentration (mg L^{-1}), q_{max} is the maximum adsorptive capacity (mg g^{-1}), K_L is the Langmuir equilibrium constant (L mg^{-1}), K_F is a constant that indicates the extent of adsorption (mg g^{-1})·(mg L^{-1})$^{-1/}$ n_F , n_F is the Freundlich intensity parameter, K_S is the Sips equilibrium constant (L mg^{-1}) and n_S the heterogeneity index.

Once the efficiency of the two processes (advanced oxidation and adsorptive) was investigated and the most adequate working conditions were determined, a third

treatment was proposed, since after the first one, undesirable by-products are often generated. For this, first the dye solution was treated via AOP and then through the adsorptive process.

2.6 Combined treatment and toxicity assessment

To reduce the final toxicity of the previously treated solution and increase dye removal efficiency, the adsorptive process was used after the AOP. The experimental times of the systems were obtained according to the kinetics of the two processes. This was determined based on the dye concentration at the characteristic λ. In addition, spectral scanning analysis was performed before and after treatments.

The toxicity of solutions treated via AOP and AOP + adsorption was evaluated with carrot seeds (*Daucus carota subsp. Sativus*). To this end, the methodology described by Santos *et al.* (2020) exposing 20 seeds to the dye solution before and after the mentioned treatments, as well as to a 3% boric acid solution (positive control) and distilled water (negative control). After an incubation period of 120 h, the relative growth indices (RGI) and germination (GI) of the seeds were determined, as described by Young *et al.* (2012).

3 RESULTS AND DISCUSSION

3.1 Spectrophotometric analysis of the acid blue dye 80

Spectral scanning analysis of the aqueous solution of the acid blue dye 80 (AA80) was performed in the range of 200 to 800 nm, using 3 different pH ranges. The spectra obtained are shown in Figure 1.

Analyzing Figure 1, the presence of three characteristic peaks of the dye solution can be seen, the 622 nm peak being related to the chromophore group and the peaks at 215 and 334 nm referring to the presence of aromatic groups and auxochromes (PAULINO; ARAÚJO; SALGADO, 2015). However, the monitoring was carried out only at

the λ of 622 and 334 nm, considering that the λ of 215 nm is close to the equipment stabilization range, presenting low reliability in the quantification.

Figure 1 – Acid blue dye 80 spectra at different pH ranges

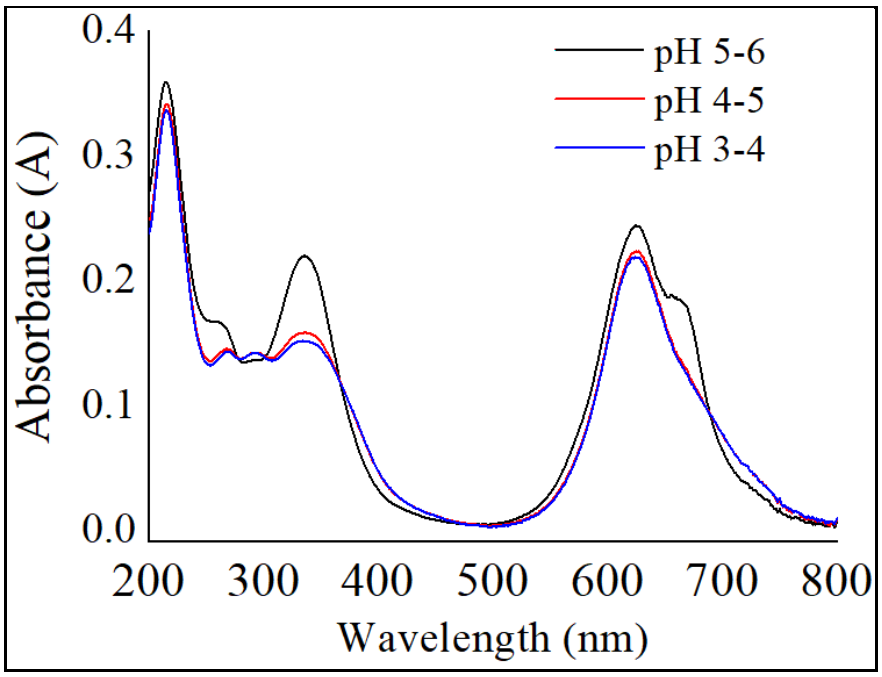

It is also observed, in Figure 1, a decay in the intensity of the peaks of 622 and 334 nm when the pH varies. This proves the existence of a cleavage of chromophore groups responsible for dye coloration, and, therefore, it was decided to build two analytical curves fixing the pH in the 3-4 range (ideal for Fenton reactions). Both curves showed correlation coefficient values ≥ 0.998, showing good linearity. From the values of LOD (2.16 and 2.22 mg L^{-1}), LOQ (2.60 and 2.75 mg L^{-1}) and CV (2.82% and 3.28%) as predicted by Harris (2001), the precision and low dispersion of data.

Possessing a methodology for detection and quantification of the AA80 dye, the treatment step was carried out using, initially, advanced oxidation processes.

3.2 Treatment using advanced oxidation processes

The degradation of the AA80 dye was evaluated by applying the photolysis process and the AOP photoperoxidation and photo-Fenton. Table 1 shows the results of the average degradation percentages obtained in each process.

Table 1– Percentage of degradation achieved with different treatment processes

Process	**Photolysis**		**Photoperoxidation**		**photo-Fenton**	
Radiation	**UV-C**	**LED**	**UV-C**	**LED**	**UV-C**	**LED**
334 nm	15.9%	0	72.7%	0	74.8%	65.2%
622 nm	7.2%	0	83.8%	0	96.7%	98.0%

By analyzing Table 1, it can be seen that the photolysis process was not able to promote the degradation of the dye, especially when using LED radiation. The photoperoxidation/UV-C system led to degradations of 72.7 and 83.8% for λ of 334 and 622 nm, respectively. However, the photoperoxidation process associated with LED radiation was also not efficient, which can be explained by the lower energy emitted by this type of radiation to perform the homolytic breakdown of H_2O_2 (NASCIMENTO JÚNIOR *et al.* 2018). With regard to the photo-Fenton process, it managed to degrade the dye under study in the two radiations analyzed, especially with regard to the chromophore group (622 nm). In this AOP, ferrous ions act as electron donors for radical systems, while hydrogen peroxide decomposes into radicals and hydroxyl ions, causing the oxidation of ferrous ions to ferric ions (SOUZA *et al.* 2010). Thus, the photo-Fenton/LED and photoperoxidation/UV-C systems went on to the optimization step of the variables [H_2O_2] and [Fe] (when applicable). The results of photoperoxidation using UV-C radiation are shown in Figure 2.

Figure 2 – Study of the influence of [H_2O_2] on the photoperoxidation/UV-C system

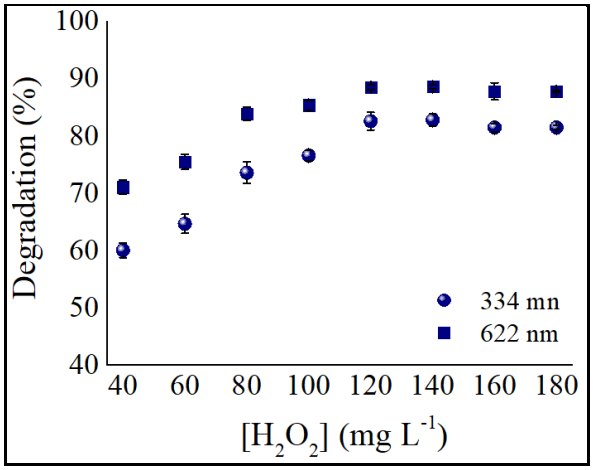

In the analysis of Figure 2, there is an increase in degradation when the concentration of H_2O_2 is increased to 120 mg L^{-1}. From this [H_2O_2] on, there is a stabilization in the degradation values for 2 evaluated wavelengths. The reduction in treatment efficiency is associated with the hydroperoxyl radical ($HO_2^{\bullet}$), formed by the reaction between the $HO^{\bullet}$ radicals and the excess of H_2O_2 in the medium (SU *et al.* 2011). Thus, the limiting concentration of H_2O_2 to treat acid blue dye 80 via photoperoxidation/UV-C was equal 120 mg L^{-1}. Once the best working condition for photoperoxidation was defined, the ideal [H_2O_2] was also determined for the photo-Fenton process in the two radiations under study (UV-C and LED) (Figure 3).

Figure 3 – Study of the influence of [H2O2] on the photo-Fenton process using radiation: (a)UV-C with [Fe] = 3 mg L^{-1} (b) LED with [Fe] = 1 mg L^{-1}. Experimental conditions: pH between 3-4, V = 50 mL, t = 60 min

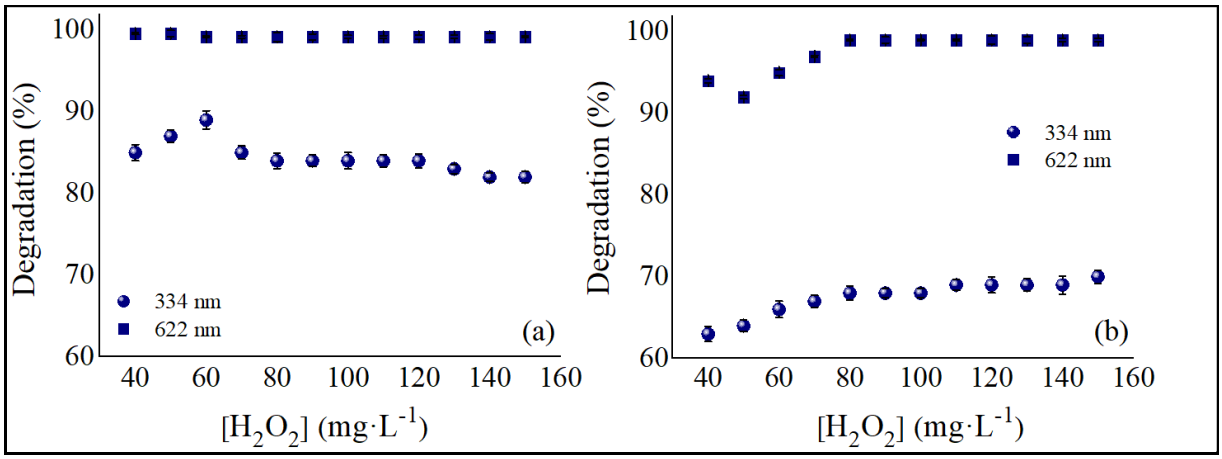

Through the analysis of Figure 3 it is possible to verify that there were no significant differences in the [H_2O_2] used, achieving a high percentage of degradation especially for the λ of 622 nm. By analyzing the radiations separately, it can be seen that for UV-C radiation (Figure 3 (a)) the increase in [H_2O_2] up to 60 mg L^{-1} favored the treatment efficiency, while using LED radiation (Figure 3 (b)), there was only a stabilization of degradation from [H_2O_2] of 90 mg L^{-1}. These results show that LED radiation exerts less influence than UV-C radiation for degradation of AA80 dye.

Nevertheless, when evaluating the acquisition and operation costs of the photo-Fenton/LED system, it is observed that is application is more advantageous in relation

to the use of the same process with UV-C radiation. This advantage is related to the difference between the average price of the LED lamp (US $ 5.55) with 10 W of power and the UV-C lamp (US $ 19.30) with 30 W of power, besides the operational cost being US $ 0.00408 an hour, using 3 10W LED bulbs and US $ 0.012 an hour using 3 UV-C bulbs (30W). It is noteworthy that the calculation of the operation cost was performed based on the photo emission values $3.75x10^3$ W cm^{-2} and $1.85x10^3$ W cm^{-2}, of the set of 3 LED and UV-C lamps, respectively, considering the average value of US $ 0.136 por kWh, established by Companhia Energética de Pernambuco (NEOENERGIA) for type B3 units.

With the ideal concentrations of oxidant for each case, the influence of iron concentration (Figure 4) on the photo-Fenton process was studied.

Figure 4 – Study of the influence of [Fe] on the photo-Fenton process using radiation: (a) UV-C with [H_2O_2] = 60 mg L^{-1} and (b) LED with [H2O2] = 90 mg L^{-1}. Experimental conditions: pH between 3-4, V = 50 mL, t = 60 min

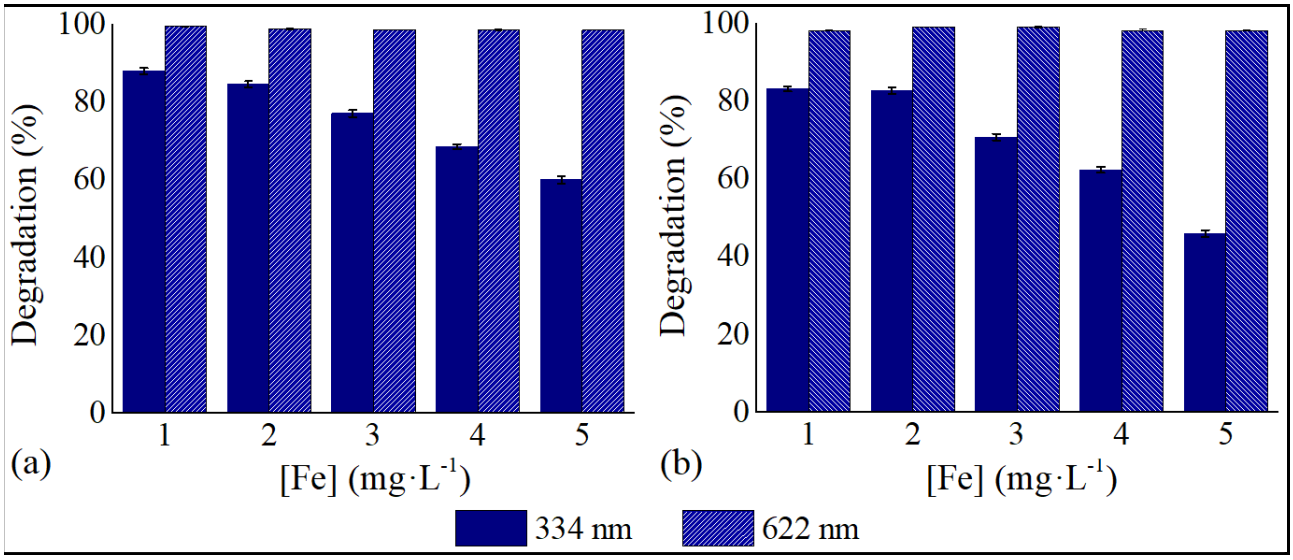

In Figure 4, it is observed that a greater efficiency of the photo-Fenton process, in the two analyzed λ, was achieved when using the smallest [Fe] for the two radiations tested. This behavior can be explained by the self-inhibition of hydroxyl radicals when there is an excess of ferrous ions (BENSALAH *et al.* 2019). A similar result was obtained by Nascimento *et al.* (2018) when treatment Reactive Gray BF-2R dye via photo-

Fenton/UV-C. The authors achieved greater treatment efficiency when using [Fe] of 1 mg L^{-1}, also using pH between 3-4.

To ensure the efficiency of the tested processes, a study of the volume variation of the treated solution was carried out using the best conditions already established. For this purpose, 50, 100, 200, 500 and 1000 mL of the dye solution were subjected to treatments, with the results shown in Figure 5.

Figure 5 – Study of volume variation for the systems: (a) photoperoxidation/UV-C (b) photo-Fenton/UV-C and (c) photo-Fenton/LED

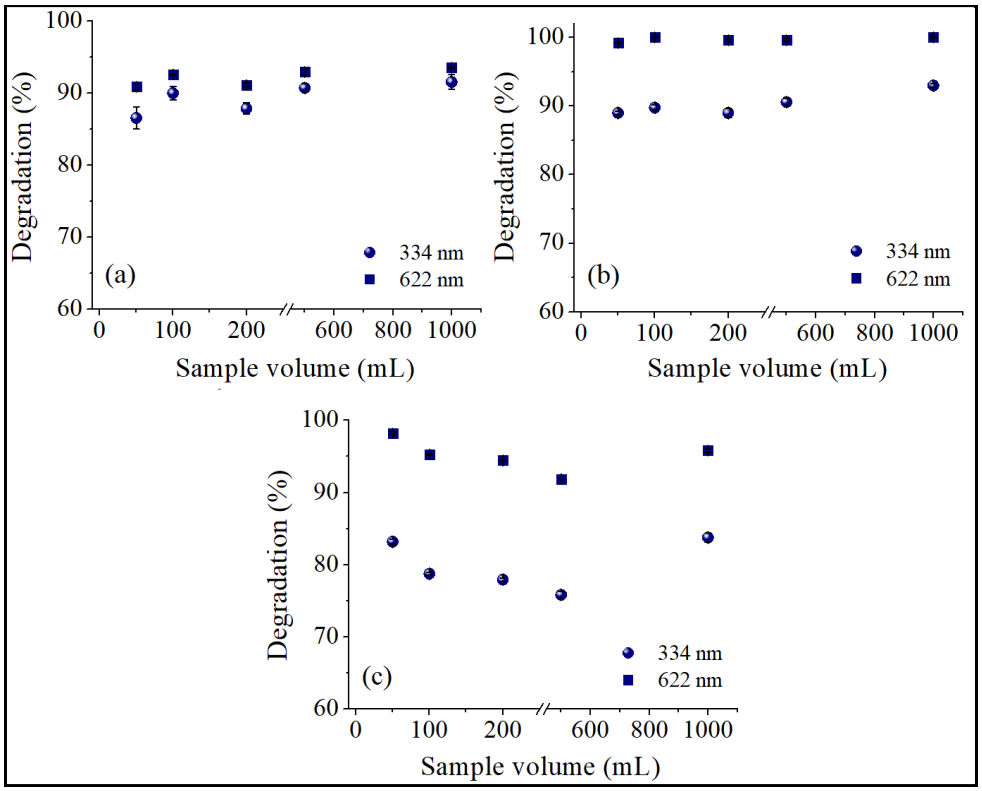

As can be seen in Figure 5, the increase in the volume of solution to be treated led to differences in degradations below 10% for the three systems evaluated. The same behavior was observed by Silva *et al.* (2020) for the solution of the dyes direct red 23 (DR23), direct red 227 (DR227) and direct orange 26 (DO26). Thus, it was possible to conduct the kinetic evaluation of the processes, using a volume of 1000 mL. The results of the kinetic study employing the best operating conditions defined for each selected system are shown in Figure 6.

Figure 6 – Degradation kinetics of the acid blue dye solution 80 using the processes: (a) photoperoxidation/UV-C with pH 5-6 and [H_2O_2] = 120 mg L^{-1} (b) photo-Fenton/UV-C with pH 3-4, [H_2O_2] = 60 mg L^{-1} and (c) photo-Fenton/LED with pH 3-4, [H_2O_2] = 90 mg L^{-1}. Experimental conditions: T = 31 ± 1ºC, [Fe] = 1 mg L^{-1} and p = 1 atm

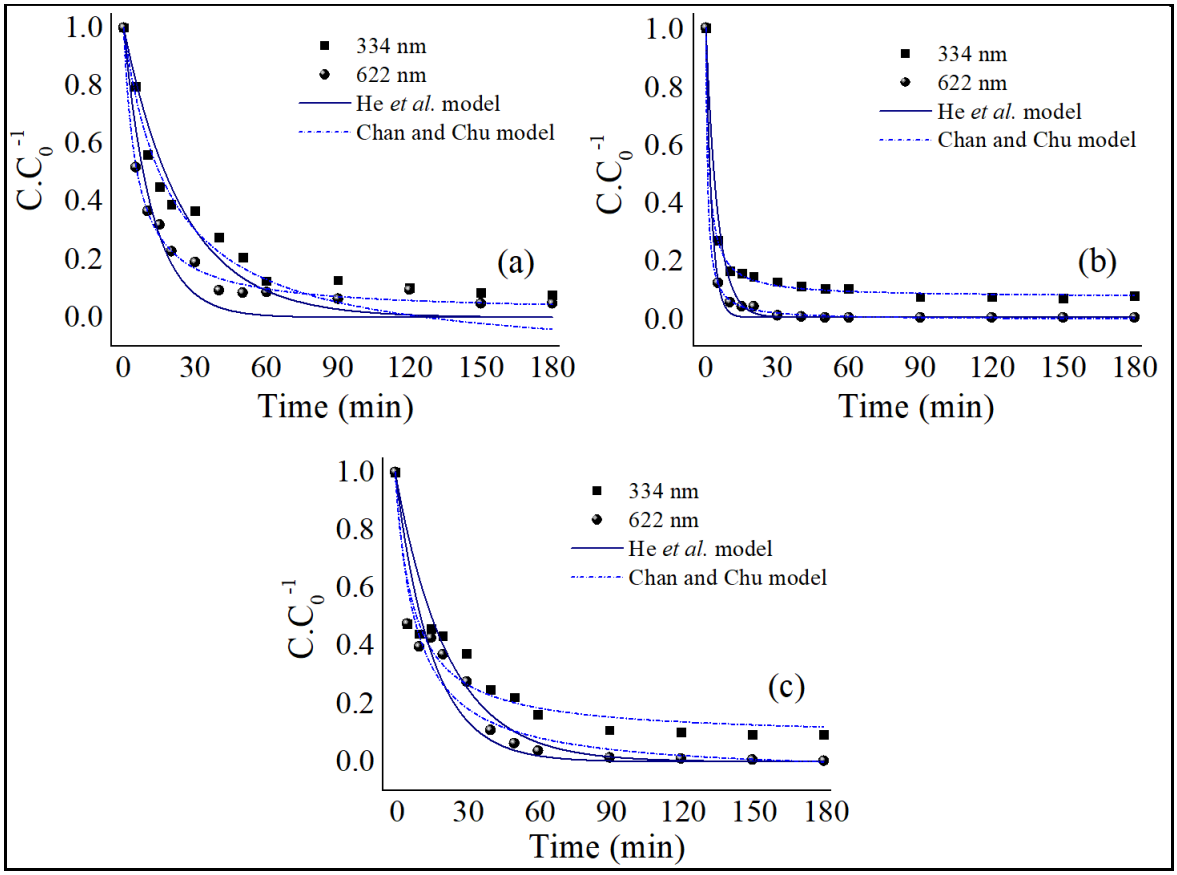

Through the analysis of Figure 6, it can be stated that for the three processes analyzed, the degradation of the AA80 dye occurs more intensely in the first 60 min of reaction, however the stabilization stage starts at different times for each of the systems. The degradation percentages obtained at the end of the process for λ 622 nm were equal 95.14, 100 and 99.62% for photoperoxidation/UV-C, photo-Fenton/UV-C, and photo-Fenton/LED, respectively. Regarding the λ of 334 nm, degradations of 92.41, 92.63 and 90.19% were achieved for the systems already mentioned, respectively. To assess the kinetic models used in more detail, Table 2 describes the parameters related to the kinetic adjustments obtained for each system.

Table 2 – Kinetic parameters of the models by Chan and Chu (2003) and He *et al.* (2016) for the different AOP

Models	Parame-ters	PP UV-C		PF UV-C		PF LED	
		334 nm	622 nm	334 nm	622 nm	334 nm	622 nm
He *et al.* (2016)	k (min^{-1})	0.04±0.01	0.08±0.01	0.21±0.04	0.40±0.02	0.04±0.01	0.06±0.01
	R^2	0.93	0.92	0.87	0.99	0.71	0.89
Chan and Chu (2003)	ρ (min)	17.01±0.14	5.66±0.38	1.44±0.09	0.71±0.034	8.25±1.67	8.25±1.35
	σ	0.87±0.01	1.02±0.01	1.07±0.01	0.99±0.01	1.09±0.05	0.95±0.04
	R^2	0.98	0.99	0.99	0.99	0.99	0.94

PP - photoperoxidation; PF- photo-Fenton

Based on the data presented in Table 2, it was possible to observe a better fit of the experimental data to the model proposed by Chan and Chu (2003), with R^2 values greater than 0.94, in all analyzed processes. On the other hand, only photoperoxidation could be described by the model proposed by He *et al.* (2016), since the systems employing the photo-Fenton AOP presented $R^2 < 0.90$ for the two monitored λ. It is also observed that for 622 nm, both processes that made use of UV-C radiation had a more accentuated degradation. This can be confirmed by the value referring to the reaction kinetics (ρ), since the lower its value, the greater the initial decay related to the evaluated wavelength (PAULINO *et al.* 2015). Once the kinetic study was completed, the removal of the AA80 dye was evaluated through the adsorptive process.

3.3 Adsorbent characterization

Determining the pH of the point of zero charge in the adsorptive process is essential to understand the surface charge of the adsorbent, which is responsible for conducting the electrostatic interactions between the material and the adsorbate (NASCIMENTO *et al.* 2014). Therefore, initially the pH_{PZC} of the prepared adsorbent was determined (Figure 7 (a)). In addition, Fourier Transform Infrared Spectroscopy (FTIR) analysis was performed, Figure 7 (b), in order to determine the functional groups, present on the surface of the adsorbent of chicken eggshell *in natura*.

Figure 7 (a) – pHPZC of chicken eggshell in natura, (b) FTIR of chicken eggshell in natura

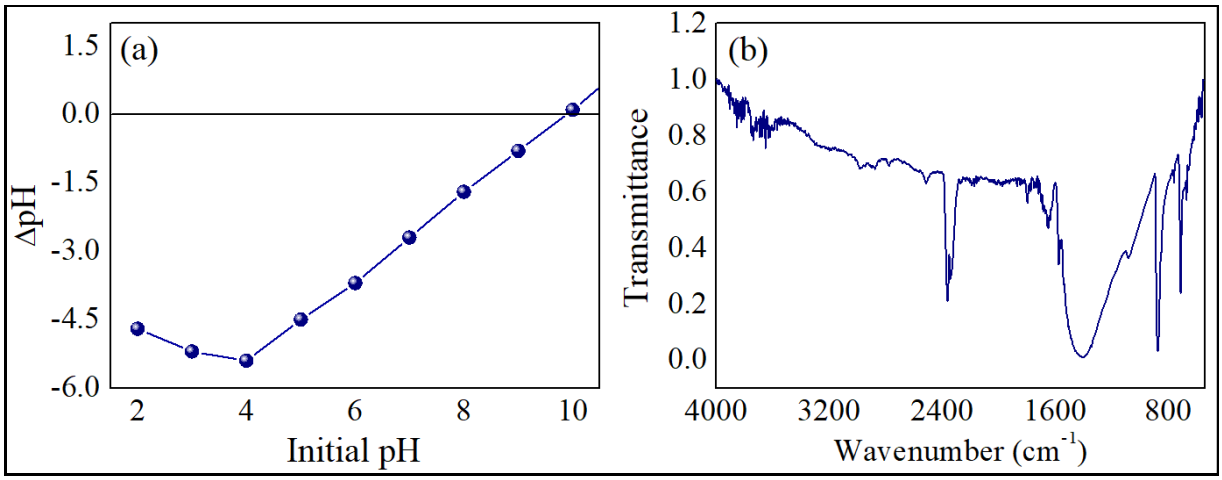

Analyzing Figure 7 (a) it is verified that the pH_{PZC} of the material *in natura* is equal to 10. Knowing that for pH values of the solution below pH_{PZC} the surface of the adsorbent will be positively charged, and that for values above pH_{PZC} the surface will be negatively charged, the adsorption of anionic species such as the dye under study, should be favored in values of pH lower than pH_{PZC} (TEMESGEN; GABBIYE; SAHU, 2018; ÇELEKLI; AL-NUAIMI.; BOZKURT, 2019).

According to the spectrum shown in Figure 8 (b), it is possible to observe the presence of bands referring to calcium carbonate at 712 cm^{-1} and 872 cm^{-1}, respectively (RODRÍGUEZ-NAVARRO *et al.* 2013). Tsai *et al.* (2006) observed bands around 743 cm^{-1} and 870 cm^{-1} related to deformations in the planes that indicate the presence of $CaCO_3$. It is also verified the presence of a band that is related to the vibration of the stretching of phosphate groups with wavelengths around 1550 – 899 cm^{-1}, in addition to the peak of 1574 cm^{-1} associated with primary amide (CHOUDHARY; KOPPALA; SWAMIAPPAN, 2015; RODRÍGUEZ-NAVARRO *et al.* 2015). On the other hand, it is also observed the presence of peaks at 1646, 1796 and 2361 cm^{-1}, referring respectively to the vibration of the primary amine, the stretching of C=O bonds of the amide groups and the maximum peak attributed to $Ca(OH)_2$ (LI *et al.* 2014; ELETTA *et al.* 2016).

After the characterization of the adsorbent material, the study of the variables of the adsorbent process was carried out.

3.4 Study of the variables for the adsorptive process: factorial design

The factorial design aimed to define the best condition for the adsorptive treatment based on the study of the particle size, pH and stirring speed variables. Thus, the data obtained were processed in the *Statistica 6.0* software, obtaining Pareto charts for each λ monitored (Figure 8) with 95% confidence level.

Figure 8 – Pareto charts obtained factorial design analysis 2^3 plus central point for λ of: a) 334 nm and b) 622 nm

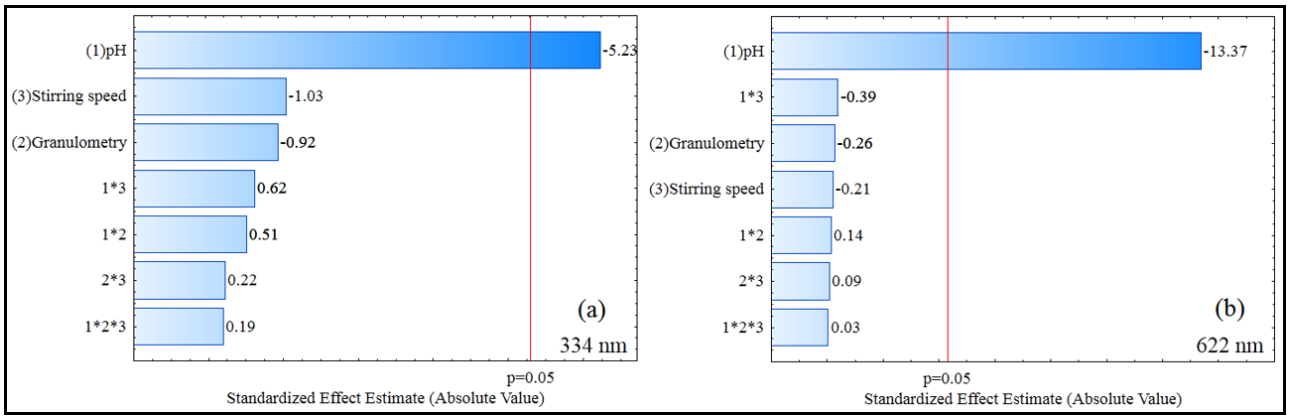

In Figure 8, it is possible to observe that only the pH variable influenced the removal of the contaminant for both analyzed wavelengths. This variable had negative values, indicating that a greater adsorptive capacity is obtained for the lowest pH level studied. In view of the non-interference of the other analyzed variables, it was decided to follow the studies using the lowest stirring speed, that is, no stirring and the largest particle size. These choices were made in order to reduce costs, since an energy source does not need to be used and use the adsorbent in the granulometric form with greater availability. With these data, the kinetic study of the adsorptive process could be carried out.

3.5 Adsorption kinetic study

Using a pH equal to 2, adsorbent particle size less than 0.9 mm and without using an energy source for stirring, the kinetic study was carried out. From the experimental data obtained, it was possible to analyze their convergence to pseudo-first order and pseudo-second order kinetic models (Figure 9).

Figure 9 – Kinetic study: experimental data and adjustments to pseudo-first order and pseudo-second order models. Experimental conditions: pH range between 2-3, without stirring and in the largest particle size of the adsorbent

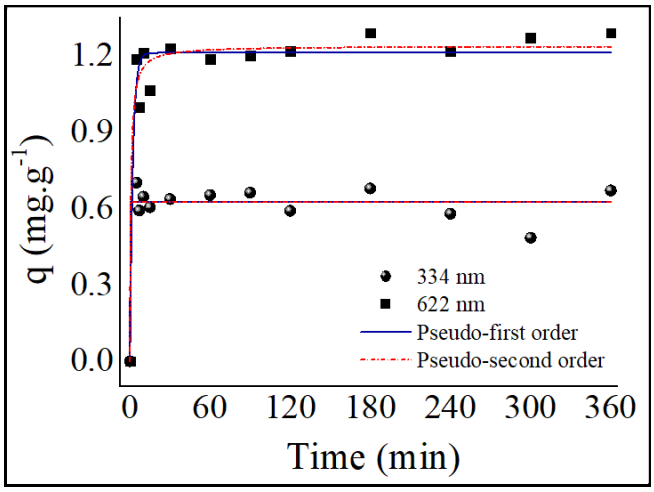

Figure 9 shows a rapid evolution of kinetics in the first 20 min, which must be associated with greater availability of active sites at the beginning of the process. This allows the contaminant to quickly coat the entire surface of the adsorbent. Then, the deceleration of the adsorption rate is started, which must occur due to the low speed in the diffusion of the dye molecules in the pores of the material used (JAAFARI *et al.* 2020). Equilibrium was reached in 30 min and presented a removal rate 62.45 and 83.22%, respectively, for λ = 334 nm and 622 nm.

As can be seen in Figure 10, the two kinetic models evaluated presented a good fir to the experimental data. The parameters of the kinetic adjustments for the batch adsorptive process are shown in Table 3.

Table 3 – Kinetic parameters for pseudo-first order and pseudo-second-order models

Models	**Parameters**	**334 nm**	**622 nm**
Pseudo-first order	q_e (mg g^{-1})	0.62 ± 0.02	1.21 ± 0.03
	k_1 (min^{-1})	462 ± 1	0.46 ± 0.13
	Sr^2	0.034	0.073
	R^2	0.91	0.94
Pseudo-second order	q_e (mg g^{-1})	0.62 ± 0.02	1.24 ± 0.03
	k_2 (g mg^{-1} min^{-1})	$1.21x10^{44}$ ± $1.47x10^{43}$	1.10 ± 0.49
	Sr^2	0.034	0.052
	R^2	0.91	0.96

From the data presented in Table 3, it is observed that the linear regression coefficients (R^2) are greater than 0.9 for the λ and models studied. Therefore, when verifying the results in relation to the λ of 334 nm, it was observed that the two models presented similar R^2 and Sr^2 values, thus demonstrating a good fit for both. In relation to the λ of 622 nm, the pseudo-second order model obtained a better fit, compared to the pseudo-first order model, as it presented a higher R^2 value and a lower Sr^2 value. Thus, it is suggested that the treatment of AA80 dye using chicken eggshell as an adsorbent follows a pseudo-second order models, which predicts the chemisorption mechanism over time until reaching the equilibrium state (YU *et al.* 2020).

Still analyzing Table 3, it is verified that the kinetic constants obtained for the λ of 334 nm presented high values, corroborating the behavior of the dye removal curve shown in Figure 10. According to Tan and Hameed (2017), the kinetic constants are inversely proportional to the time it takes system to reach equilibrium. Thus, the faster the adsorption, the greater the constants. With the results obtained for the adsorption kinetics, it was passed to the step of evaluating the equilibrium of the adsorptive process.

3.6 Adsorption equilibrium study

It was possible to analyze the adsorption behavior of the acid blue dye 80 on the adsorbent *in natura* by adjusting the experimental data to the models isotherms of Langmuir, Freundlich and Sips isotherms, from equilibrium study that was carried out in 30 min. Thus, the isotherms for each studied λ were obtained as can be seen in Figure 10.

From Figure 10, a better fit can be observed for the Langmuir and Sips models, which can be confirmed by the parameter values obtained from the isotherm model fits that are shown in Table 4.

Figure 10 – Fitting the isotherms for the Langmuir, Freundlich and Sips models for the λ of: a) 334 nm and b) 622 nm

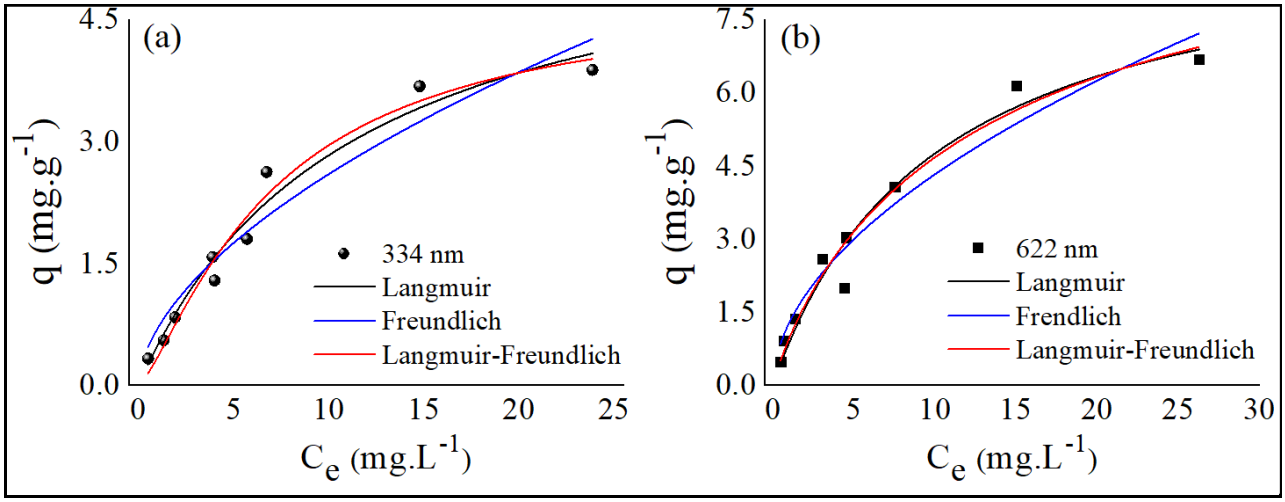

Table 4 – Isotherm parameters for models of Langmuir, Freundlich and Sips

Models	Parameters	334 nm	622 nm
Langmuir	q_{max} (mg g^{-1})	6.00 ± 0.66	9.50 ± 1.04
	K_L (L mg^{-1})	0.09 ± 0.02	0.10 ± 0.02
	Sr^2	0.40	1.36
	R^2	0.97	0.96
Freundlich	K_F (mg g^{-1})·(mg L^{-1})$^{-1/n_F}$	0.70 ± 0.12	1.28 ± 0.19
	n_F	1.76 ± 0.21	1.89 ± 0.20
	Sr^2	0.84	1.95
	R^2	0.93	0.94
Sips	q_{max} (mg g^{-1})	4.84 ± 0.77	10.71 ± 4.14
	K_S (L mg^{-1})	0.08 ± 0.02	0.10 ± 0.03
	n_S	0.77 ± 0.17	1.12 ± 0.32
	Sr^2	0.33	1.32
	R^2	0.97	0.96

According to Table 4, the experimental data presented a good fit to the three equilibrium models evaluated, with values of $R^2 > 0.90$. However, the Langmuir and Sips models presented the highest R^2 values and the lowest Sr^2, indicating that the interaction between the contaminant and the adsorbent can be represented by these two models. The Langmuir isotherm described adsorption as a monolayer covering in which the adsorption rate limiting factor is the availability of active sites (YU *et al.* 2020). On the other hand, the Sips model is related to the limiting behavior of its equation,

that is, for low concentrations of adsorbate, the equation effectively reduces to a Freundlich isotherm and thus does not obey Henry's law. For high concentrations, a monolayer adsorption capacity, characteristic of the Langmuir isotherm is predicted (HO; PORTER; McKAY, 2002). Thus, the adsorption of the AA80 dye by the hen's eggshell can be represented by the Langmuir and Sips models.

After completing the study of the process of removing the dye AA80 via adsorption, the treatment step was carried out by combining this process with the AOP.

3.7 Advanced oxidation process followed by adsorption

Given the above mentioned studies, the photoperoxidation/UV-C (PP/UV-C) and photo-Fenton/LED (PF/LED) systems showed the best results in terms of cost/benefit. Despite the good degradation efficiency of these systems, AOP can generate, during the treatment, intermediate compounds with greater toxicity than the initial compounds. Thus, after the completion of the systems using the AOP, the treated solution was submitted to the adsorptive process (ADS), using the raw chicken eggshell adsorbent, in order to remove these possible compounds generated in the process. Thus, based on the results of the kinetic evaluations and identified the point of stabilization of each process, the combined study (AOP/ADS) was carried out by submitting the AA80 solution to 90 min of the AOP and 30 min of adsorption, under the optimal conditions of each system. The results of treatments after the AOP and after the combined (AOP/ADS) are shown in Figure 11.

From Figure 10, it is possible to observe that for the PP/UV-C+ADS and PF/LED+ADS systems there is a reduction in the intensity of the peaks studied when compared to the systems that made exclusive use of the treatment via AOP. For the λ = 334 nm, the treatment efficiency before and after the combined system increased from 90.27% to 96.43% (PP/UV-C system) and from 88.68% to 97.12% (PF/LED system). While for λ = 622 nm the efficiency remained around 99% for both systems. This shows that the combined use of the two processes can increase the final quality of the treated matrix.

Figure 11 – Acid blue dye 80 spectra after AOP and AOP+ADS treatments

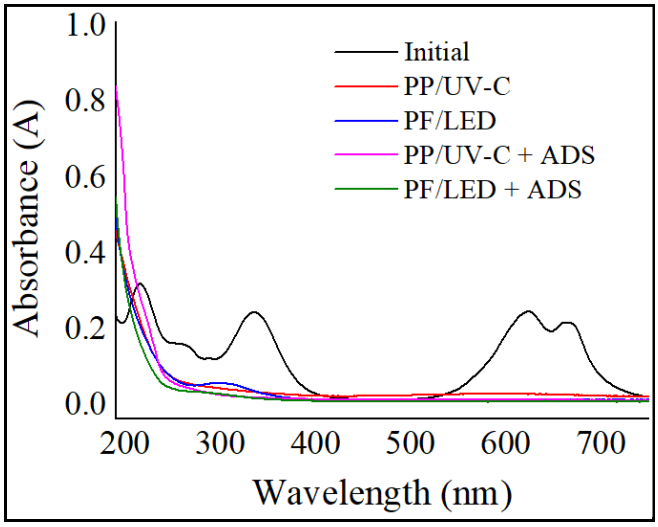

Then, toxicity tests were carried out for carrot seeds. In the positive control assays, no germination was observed. The data obtained for the other samples are shown in Table 5.

Table 5 – GI(%) and RGI values for carrot seed (*Daucus carota subsp. Sativus)* in different systems

Parameters	GI (%)	RGI
Negative control (water)	100.00	1.00
Initial Solution	30.78	0.55
Photoperoxidation/ UV-C	61.30	0.64
Photoperoxidation/UV-C + ADS	65.47	0.71
Photo-Fenton/LED	18.84	0.29
Photo-Fenton/LED + ADS	60.08	0.70

ADS - adsorption

When analyzing the germination and growth indexes of carrot seeds (Table 5), it can be seen that the initial solution of the AA80 dye and the treated solutions showed toxicity, as the RGI values were lower than the negative control. Among the proposed treatments, the photo-Fenton/LED system was the most harmful to seeds. The adsorptive process combined with this AOP reduced the toxicity, raising the RGI by 58%.

However, although the association of processes has allowed a significant reduction in the toxicity of the toxicity of the dye solution by increasing the germination

and growth indices, according to Young *et al.* (2012), it did not completely decrease toxicity. This is due to the fact that the RGI remained below 0.8.

4 CONCLUSIONS

In view of the study carried out, it was observed that the processes of photoperoxidation and photo-Fenton, using UV-C and LED radiation, respectively, were efficient in the degradation of the acid blue dye 80 (AA80) in aqueous solution. Despite the high levels of degradation of the contaminant achieved, the AA80 dye solutions showed toxicity to the organism tested before and after treatment by AOP. Therefore, the adsorptive study was used in combination with the AOP, aiming to improve the final quality of the post-treatment solution. The chicken eggshell, *in natura*, was used as a biosorbent in view of the application of this residue, as well as its high efficiency in the removal of organic and inorganic compounds. The combined treatment (AOP+ADS) showed greater removal of the studied pollutant, improving the toxicity indexes when compared to the treatment by isolated AOP. Thus, the combination of processes proved to be a viable alternative for the treatment of textile dyes, as well as the use of agro-industrial waste as an adsorbent.

ACKNOWLEDGEMENTS

CAPES, NUQAAPE/FACEPE (FACEPE, APQ-0346-1.06/14 process) and FADE/UFPE

REFERENCES

AMORIM, N. D. O.; NASCIMENTO, G. E.; CHARAMBA, L. V. C.; SANTANA, R. M. R.; SILVA, P. M.; NAPOLEÃO, T. H.; NAPOLEÃO, D. C. Direct red 83 textile dye degradation using photoperoxidation and photo-Fenton: kinetic studies, toxicity and neural networks modeling. **Ciência e Natura**, v. 42, 2020. doi.org/10.5902/2179460X40986

BANASCHIK, R.; JABLONOWSKI, H.; BEDNARSKI, P. J.; KOLB, J. F. Degradation and intermediates of diclofenac as instructive example for decomposition of recalcitrant pharmaceuticals by hydroxyl radicals generated with pulsed corona plasma in water. **Journal of Hazardous Materials**, v. 342 p. 651–660, 2018. doi.org/10.1016/j.jhazmat.2017.08.058

BENSALAH, N.; DBIRA, S.; BEDOUI, A. Mechanistic and kinetic studies of the degradation of diethyl phthalate (DEP) by homogeneous and heterogeneous Fenton oxidation. **Environmental Nanotechnology, Monitoring & Management**, v. 11, p. 100224, 2019. doi.org/10.1016/j.enmm.2019.100224

BORTOTI, A. A.; ROSA, M. F.; BARICCATTI, R. A.; LOBO, V. S. Avaliação do processo foto-Fenton na descoloração de um corante têxtil comercial. **Semina: Ciências Exatas e Tecnológicas**, v. 37, n.1, p. 81-90, 2016. doi.org/10.5433/1679-0375.2016v37n1p81

BRITO, N. N.; SILVA, V. B. M. Processo oxidativo avançado e sua aplicação ambiental, **Revista Eletrônica de Engenharia Civil**, v. 1, n.3, p. 36-47, 2012.

BRUCKMANN, F. D. S.; VIANA, A. R.; TONEL, M. Z.; FAGAN, S. B.; GARCIA, W. J. D. S.; OLIVEIRA, A. H. D.; DORNELES, L. S.; MORTARI, S. R.; SILVA, W. L.; SILVA, I. Z.; RHODEN, C. R. B. (2022) Influence of magnetite incorporation into chitosan on the adsorption of the methotrexate and in vitro cytotoxicity. **Environmental Science and Pollution Research**, 29, 70413–70434, 2022. doi.org/10.1007/s11356-022-20786-x

ÇELEKLI, A.; AL-NUAIMI, A. I.; BOZKURT, H. Adsorption kinetic and isotherms of Reactive Red 120 on Moringa oleifera seed as an eco-friendly process. **Journal of Molecular Structure**, v. 1195, p. 168-178, 2019. doi.org/10.1016/j.molstruc.2019.05.106

CHAN, K. H.; CHU, W. Modeling the reaction kinetics of Fenton's process on the removal of atrazine. **Chemosphere**, v. 51, n. 4, p. 305–311, 2003. doi.org/10.1016/s0045-6535(02)00812-3

CHOUDHARY, R.; KOPPALA, S.; SWAMIAPPAN, S. Bioactivity studies of calcium magnesium silicate prepared from eggshell waste by sol-gel combustion synthesis**. Journal of Asian Ceramic Societies**, v. 3, p. 173–177, 2015. doi.org/10.1016/j.jascer.2015.01.002

DIAZ-MUÑOZ, G.; MIRANDA, I. L.; SARTORI, S. K.; DE REZENDE, D. C.; DIAZ, M. A. N. Anthraquinones: An Overview. **Studies in Natural Products Chemistry**, v. 58, p. 313–338, 2018. doi.org/10.1016/B978-0-444-64056-7.00011-8

ELETTA, O. A. A.; AJAYI, O. A.; OGUNLEYE, O. O.; AKPAN, I. C. Adsorption of cyanide from aqueous solution using calcinated eggshells: equilibrium and optimisation studies. **Journal of Environmental Chemical Engineering**, v. 4, p. 1367–1375, 2016. doi.org/doi:10.1016/j.jece.2016.01.020

FERRAZ, E. R. A.; UMBUZEIRO, G. A.; DE-ALMEIDA, G.; CALOTO-OLIVEIRA, A.; CHEQUER, F. M. D.; ZANONI, M. V. B.; DORTA, D. J.; OLIVEIRA, D. P. Differential toxicity of Disperse Red 1 and Disperse Red 13 in the Ames test, HepG2 cytotoxicity assay, and Daphnia acute toxicity test. **Environmental Toxicology**, v. 26, n. 5, p. 489-497, 2011. doi.org/10.1002/tox.20576

HARRIS, D. C. **Análise química quantitativa**. LTC, Rio de Janeiro, 2001.

GHIBATE, R.; SENHAJI, O.; TAOUIL, R. Kinetic and thermodynamic approaches on Rhodamine B adsorption onto pomegranate peel. **Case Studies in Chemical and Environmental Engineering**, V 3:100078. 2021. doi.org/10.1016/j.cscee.2020.100078

HE, J.; YANG, X.; MEN, B.; WANG, D. Interfacial mechanisms of heterogeneous Fenton reactions catalyzed by iron-based materials: A review. **Journal of Environmental Sciences**, v. 39, p. 97-109, 2016. doi.org/10.1016/j.jes.2015.12.003

HE, Y.; SUTTON, N. B.; RIJNAARTS, H. H. H.; LANGENHOFF, A. A. M. Degradation of pharmaceuticals in wastewater using immobilized TiO_2 photocatalysis under simulated solar irradiation. **Applied Catalysis B: Environmental**, v. 182, p. 132-141, 2016. doi.org/10.1016/j.apcatb.2015.09.015

HEVIRA, L.; RAHMI, A.; ZEIN, R.; ZILFA, Z.; RAHMAYENI, R. The fast and of low-cost-adsorbent to the removal of cationic and anionic dye using chicken eggshell with its membrane. **Mediterranean Journal of Chemistry**, v.10 n.3 p. 294-301.2020 doi.org/10.13171/mjc02003261271lh

HO, Y. S.; PORTER, J. F.; MCKAY, G. Equilibrium Isotherm Studies for the Sorption of Divalent Metal Ions onto Peat: Copper, Nickel and Lead Single Component Systems. **Water, Air, and Soil Pollution**, v. 141, p. 1–33, 2002. doi.org/10.1023/A:1021304828010

Instituto Nacional de Metrologia. Normalização e Qualidade Industrial – INMETRO (2016) DOC-CGCRE-008: Orientação sob validação de métodos analíticos.

JAAFARI, J.; BARZANOUNI, H.; MAZLOOMI, S.; FARAHANI, N. A. A.; SHARAFI, K.; SOLEIMANI, P.; HAGHIGHAT, G. A. Effective adsorptive removal of reactive dyes by magnetic chitosan nanoparticles: Kinect, isothermal studies and response surface methodoly. **Internacional Journal of Biological Macromolecules**, v. 164, p. 344-355, 2020. doi.org/10.1016/j.ijbiomac.2020.07.042

KIM, E.; CHOI, J. Synthesis of cationized anthraquinone dyes and their dyeing properties for *meta*-aramid fiber. **Fibers and Polymers**, v. 14, n. 12, p. 2054–2060, 2013. doi.org/10.1007/s12221-013-2054-7

LALNUNHLIMI, S.; KRISHNASWAMY, V. Decolorization of azo dyes (Direct Blue 151 and Direct Red 31) by moderately alkaliphilic bacterial consortium. **Brazilian Journal of Microbiology**, v. 47, p. 39-46, 2016. doi.org/10.1016/j.bjm.2015.11.013

LI, Y.; WANG, L.; WU, L.; ZHANG, X.; LI, X.; GUO, Z.; LI, H.; IORQUE, P.; SHUANGYING, G.; ZHANG, J. Bio-mimetic drug delivery systems designed to help the senior population reconstruct melatonin plasma profiles similar to those of the healthy younger population. **Acta Pharmaceutica Sinica B**, v. 4, p. 60-66, 2014. doi.org/10.1016/j.apsb.2013.12.006

MEILI, L.; LINS, P. V. S.; COSTA, M. T.; ALMEIDA, R. L.; ABUD, A. K. S.; SOLETTI, J. I.; DOTTO, G. L.; TANABE, E. H.; SELLAOUI, L.; CARVALHO, S. H. V.; ERTO, A. Adsorption of methylene blue on agroindustrial wastes: experimental investigation and phenomenological modelling**. Progress in biophysics and molecular biology**, v.141, p. 60-71, 2019. doi.org/10.1016/j.pbiomolbio.2018.07.011

MORAES, N. F. S.; SANTANA, R. M. R.; GOMES, R. K. M.; SANTOS JÚNIOR, S. G.; LUCENA, A. L. A.; ZAIDAN, L. E. M. C.; NAPOLEÃO, D. C. Performance verification of different advanced oxidation processes in the degradation of the dye acid violet 17: reaction kinetics, toxicity and degradation prediction by artificial neural networks. **Chemical Papers**, v. 75, p. 539-552, 2020. doi.org/10.1007/s11696-020-01325-9

MUTHUPRIYA, P.; MUGILAN, M.; SIVAKUMAR, K.; Decolourization efficiency of textile dyes using peroxidase enzyme extracted from Raphanus sativus L. and its optimization studies. **Internacional Journal of Current Research in Biosciences and Plant Biology**, v. 3, n. 11, 79-84, 2016. dx.doi.org/10.20546/ijcrbp.2016.311.012

GIROLETTI, C. L.; MENEZES, J. C.; LAPOLLI, F. R.; NAGEL-HASSEMER, M. E.; Processo UV/H2O2 aplicado como pós-tratamento de águas residuárias da indústria de papel e celulose. **Revista DAE**, v. 66, n. 209, p 99-107, 2018. DOI: 10.4322/dae.2017.018

NASCIMENTO, G. E. DO; CAVALCANTI, V. O. M.; SANTANA, R. M. R.; SALES, D. C. S.; RODRÍGUEZ-DÍAZ, J. M.; NAPOLEÃO, D. C.; DUARTE, M. M. M. B. Degradation of a Sunset Yellow and Tartrazine Dye Mixture: Optimization Using Statistical Design and Empirical Mathematical Modeling. **Water, Air, and Soil Pollution**, v. 231, n. 254, 2020. doi.org/10.1007/s11270-020-04547-5

NASCIMENTO, G. E. DO; NAPOLEÃO, D. C.; AGUIAR SILVA, P. K. DE; ROCHA SANTANA, R. M. DA; BASTOS, A. M. R.; ZAIDAN, L. E. M. C.; MOURA, M. C. DE; COELHO, L. C. B. B.; DUARTE, M. M. M. B. Photo-Assisted Degradation, Toxicological Assessment, and Modeling Using Artificial Neural Networks of Reactive Gray BF-2R Dye. **Water, Air, and Soil Pollution**, v. 229, n. 12, 2018 doi.org/10.1007/s11270-018-4028-2

NASCIMENTO, R. F.; LIMA, A. C. A.; VIDAL, C. B.; MELO, D. Q., RAULINO, G. S. C. **Adsorção**: aspectos teóricos e aplicações ambientais. 1 ed. Fortaleza: UFC, 255, 2014.

PAULINO, T. R. S.; ARAÚJO, R. S.; SALGADO, B. C. B. Estudo de oxidação avançada de corantes básicos via reação Fenton (Fe^{2+}/H_2O_2). **Engenharia Sanitaria e Ambiental**, v. 20, n. 3, p. 347-352, 2015. doi.org/10.1590/S1413-41522015020000111627

PRIAC, A.; BADOT, P. M.; CRINI, G. Treated wastewater phytotoxicity assessment using Lactuta sativa: focus on germination and root elongation test parameters. **Comptes Rendus Biologies**., v. 340, n. 3, p. 188–194, 2017. doi.org/10.1016/j.crvi.2017.01.002

RAMOS, R. O.; ALBUQUERQUE, M. V. C.; LOPES, W. S.; SOUSA, J. T.; LEITE, V. D. Degradation of indigo carmine by photo-Fenton, Fenton, H_2O_2/UV-C and direct UV-C: Comparison of pathways, products and kinetics. **Journal of Water Process Engineering**, v. 37, p. 101535, 2020. doi.org/10.1016/j.jwpe.2020.101535

RATANAPONGLEKA, K.; PHETSOM, J. Decolorization of Synthetic Dyes by Crude Laccase from Lentinus polychrous. **Internacional Journal of Chemical Engineering and Applications**, v. 5, p. 26-30, 2014. doi.org/10.7763/IJCEA.2014.V5.345

RODRÍGUEZ-NAVARRO, A. B.; DOMÍNGUEZ-GASCA, N.; MUÑOZ, A.; ORTEGA-HUERTAS, M. Change in the eggshell cuticle with hen and egg freshness. **Poultry Science**, v. 92, p. 3026–3035, 2013.

RODRÍGUEZ-NAVARRO, A. B.; MARIE, P.; NYS, Y.; HINCKE, M. T.; GAUTRON, J. Amorphous calcium carbonate controls avian eggshell mineralization: A new paradigm for understanding rapid eggshell calcification. **Journal of Structural Biology**, v. 190, p. 291-303, 2015. doi.org/10.1016/j.jsb.2015.04.014

SILVA, J. C.; SANTANA, R. M. R.; NASCIMENTO, G. E.; LUCENA, A. L. A.; SILVA, A. M. R. B.; SÁ, J. L. F.; MELO, A. M. M. A.; NAPOLEÃO, D. C.; DUARTE, M. M. M. B. Evaluation of the degradation potential of different advanced oxidation processes for a textile dye mixture: a kinetic study with mathematical modeling and toxicological tests. **Ciência e Natura**, v. 42, 2020. doi.org/10.5902/2179460X39776

SOUZA, E. J.; NEVES, N. S. D. C. S., GOMES, R. K. D. M., SANTOS JÚNIOR, S. G. D., CHARAMBA, L. V. C., CAMPOS, N. F., NAPOLEÃO, D. C. Treatment of textile dyes using advanced oxidative and adsorptive processes individually and combined: study of the operational parameters, kinetic and adsorptive equilibrium. **Water Science Technology**, v. 82, n. 7, p. 1327-1338, 2020. doi.org/10.2166/wst.2020.415

SOUZA, J. L.; HOLANDA, C. A.; AIRES, A. M. L.; ALMEIDA, T. R.; OLIVEIRA, E. S.; ROCHA, M. B. C.; COSTA, A. N. Potentialities of Eichhornia azurea (water hyacinth) in the removal of the turquoise textile dye remazol in aqueous medium: Study of the kinetic mechanisms of adsorption. **Brazilian Journal of Development**, v. 6, p. 76037-76053, 2020. doi.org/10.34117/bjdv6n10-142

SOUZA, S. J. O.; LOBO, T. M.; SABINO, A. L. O.; OLIVEIRA, S. B.; COSTA, O. S. Decomposição dos antirretrovirais lamivudina e zidovudina pelo processo fotofenton assistido no efluente de indústria farmoquímica. **Revista Processos Químicos**, v. 4, n.7, p. 59-67, 2010. doi.org/10.19142/rpq.v4i7.108

TAN, K. L.; HAMEED, B. H. Insight into the adsorption kinetics models for the removal of contaminants from aqueous solutions. **Journal of the Taiwan Institute of Chemical Engineers**, v. 74, p. 25–48 2017. doi.org/10.1016/j.jtice.2017.01.024

TEMESGEN, F.; GABBIYE, N.; SAHU, O. Biosorption of Reactive Red Dye (RRD) on Activated Surface of Banana and Orange Peels: Economical Alternative for Textile Effluent. **Surfaces and Interfaces**, v. 12, p. 151-159, 2018. doi.org/10.1016/j.surfin.2018.04.007

TSAI, W. T.; YANG, J. M.; LAI, C. W.; CHENG, Y. H.; LIN, C. C.; YEH, C. W. Characterization and adsorption properties of eggshells and eggshell membrane. **Bioresource Technology**, v. 97, p. 488-493, 2006. doi.org/10.1016/j.biortech.2005.02.050

VIDOVIX, T. B.; JANUÁRIO, E. F. D.; BERGAMASCO, R.; VIEIRA, A. M. S. Evaluation of agro-industrial residue functionalized with iron oxide magnetic nanoparticles for chloroquine removal from contaminated water. **Materials Letters**, v.326:132915, 2022. doi.org/10.1016/j.matlet.2022.132915

WANG, X.; JIANG, C.; HOU, B.; WANG, Y.; HAO, C.; WU, J. Carbon composite lignin-based adsorbents for the adsorption of dyes. **Chemosphere**, v.206, p.587–596, 2018. doi.org/10.1016/j.chemosphere.2018.04.183

WU, T.; YANG, G.; CAO, J.; XU, Z.; JIANG, X. Activation and adsorption mechanisms of methylene blue removal by porous biochar adsorbent derived from eggshell membrane. **Chemical Engineering Research and Design**, v.188, p. 330-341, 2022. doi.org/10.1016/j.cherd.2022.08.042

XIONG, R.; LU, Z.; TANG, Q.; HUANG, X.; RUAN, H.; JIANG, W.; CHEN, Y.; LIU, Z.; KANG, J.; LIU, D. UV-LED/chlorine degradation of propranolol in water: degradation pathway and product toxicity. **Chemosphere**, v. 248, p. 125957, 2020. doi.org/10.1016/j.chemosphere.2020.125957

YIN, R.; SHANG, C. Removal of micropollutants in drinking water using UV-LED/chlorine advanced oxidation process followed by activated carbon adsorption. **Water Research**, v. 185, p. 116297, 2020. doi.org/10.1016/j.watres.2020.116297

YOUNG, B. J.; RIERA, N. I.; BEILY, M. E.; BRES, P. A.; CRESPO, D. C.; RONCO A. E. Toxicity of the effluent from an anaerobic bioreactor treating cereal residues on Lactuca sativa. **Ecotoxicology and Environmental Safety**, v. 76, n. 1, p. 182–186, 2012. doi.org/10.1016/j.ecoenv.2011.09.019

YU, K. L.; LEE, X. J.; ONG, H. C.; CHEN, W.; CHANG, J.; LIN, C.; SHOW, P. L.; LING, T. C. Adsorptive removal of cationic methylene blue and anionic Congo red dyes using wettorrefied microalgal biochar: equilibrium, kinetic and mechanism modeling. **Environmental Pollution**, v. 272, p. 115986, 2020. doi.org/10.1016/j.envpol.2020.115986

ZAIDAN, L. E.; CARNEIRO, M.; PINHEIRO, R. B.; SANTANA, R.; VIEIRA, L.; CHARAMBA, C.; CARLA, D.; LINS, V. Evaluation of Efficiency of Advanced Oxidative Process in Degradation of 2-4 Dichlorophenol Employing Uv-C Radiation Reator. **Revista Eletrônica em Gestão, Educação e Tecnologia Ambiental**, v. 21, n. 2, p. 147–157, 2017. https://doi.org/10.5902/2236117027766

Authorship contributions

1 – Daniella Carla Napoleão

Doutorado em Engenharia Química pela Universidade Federal de Pernambuco (2015). professora Adjunta C II da Universidade Federal de Pernambuco.
https://orcid.org/0000-0002-2760-562X • daniella.napoleao@ufpe.br
Contribuition: Conceptualization, Supervision, Writing – review & editing

2 – Tássia Santos Gonçalves
Cursando a Graduação em Licenciatura em Química na Universidade Federal de Pernambuco, concluindo curso técnico em química industrial no Instituto Federal de Pernambuco.
http://lattes.cnpq.br/7496855948392050 • Tássia.S.Gonçalves@ufpe.br
Contribuition: Conceptualization, Supervision, Writing – review & editing

3 – Naiana Santos da Cruz Santana Neves
Doutoranda pelo Programa de Pós-Graduação em Engenharia Química da Universidade Federal de Pernambuco.
https://orcid.org/0000-0001-8494-8058 • naiana.santana@ufpe.br
Contribuition: Investigation, Methodology

4 – Vanessa de Oliveira Marques Cavalcanti
mestranda em engenharia química pela Universidade Federal de Pernambuco.
https://orcid.org/0000-0001-8200-9065 • vanessaoliveiramcavalcanti@gmail.com
Contribuition: Formal Analysis, Methodology

5 – Marina Gomes Silva
Doutoranda pelo Programa de Pós-Graduação em Engenharia Química da Universidade Federal de Pernambuco.
https://orcid.org/0000-0002-8835-7308 • marina.g.silva@hotmail.com
Contribuition: Methodology, Writing – original draft

6 – Ingrid Larissa da Silva Santana
Doutoranda pelo Programa de Pós-Graduação em Engenharia Química da Universidade Federal de Pernambuco.
https://orcid.org/0000-0001-8545-6637 • santanasingrid@gmail.com
Contribuition: Resources, Writing – review & editing

7 – Rayany Magali da Rocha Santana
Doutoranda pelo Programa de Pós-Graduação em Engenharia Química da Universidade Federal de Pernambuco.
https://orcid.org/0000-0001-5313-9426 • rayanymagalirocha@gmail.com
Contribuition: Data Curation, Visualization, Writing – review & editing

8 – Alex Leandro Andrade de Lucena
Doutor em Engenharia Química pela Universidade Federal de Pernambuco.
https://orcid.org/0000-0001-5054-4434 • lucenaalex3@gmail.com
Contribuition: Investigation, Writing – review & editing

9 – Graziele Elisandra do Nascimento
Doutora pelo em Engenharia Química. Atualmente é pesquisadora e aluna de pós-doutorado do Programa de Pós-Graduação em Engenharia Química da Universidade Federal de Pernambuco, com bolsa de fixação de pesquisador pela Fundação de Amparo a Ciência e Tecnologia de Pernambuco
https://orcid.org/0000-0002-8691-4406 • grazielen@yahoo.com.br
Contribuition: Formal Analysis, Supervision

How to quote this article

NAPOLEÃO, D. C. .; GONÇALVES, T. S.; NEVES, N. S. da C. S.; CAVALCANTI, V. de O. M.; SILVA, M. G.; SANTANA, I. L. da S.; SANTANA, R. M. da R.; LUCENA, A. L. A. de; NASCIMENTO, G. E. do. Association of advanced oxidative and adsorptive processes for dye treatment in the sanitizer industry: kinetic, equilibrium and toxicity evaluation. **Revista Eletrônica em Gestão, Educação e Tecnologia Ambiental**, Santa Maria, v. 26, e10, 2022. Available from: https://doi.org/ 10.5902/2236117066989